Available online at www.elixirpublishers.com (Elixir International Journal)

Computational Physics

Elixir Comp. Phys. 104 (2017) 45799-45807

ISSN: 2229-712X

Vibrational spectroscopic and molecular docking studies of 5-Chloro-2-Hydroxy 3-Nitropyridine

L.Bhuvaneswari[1,*], U.Sankar[2], S.MeenakshiSundar[3] and G.John James[4]

[1]Department of Physics, N.K.R.Government Arts College for women, Namakkal-637001 T.N. India.

[2]Department of Physics, Sri K.G.S. Arts College, Srivaikuntam-628601 T.N. India.

[3] Department of Physics, Sri Paramakalyani College, Alwarkurichi-627412 T.N. India.

[4] Department of Physics, Government Arts College, Trichy -022. T.N. India.

ARTICLE INFO

Article history:

Received: 27 January 2017;

Received in revised form:

27 February 2017;

Accepted: 8 March 2017;

Keywords

FTIR,
FT-Raman,
HF and DFT,
HOMO-LUMO,
Mulliken charges,
Molecular docking.

ABSTRACT

In this study, the Fourier Transform infrared (FT-IR) and FT-Raman spectra of 5-chloro-2-Hydroxy-3-Nitro Pyridine (CHNP) have been recorded in the range 4000-400 and 3500-50 cm^{-1}respectively. The quantum mechanical calculations of energies, optimized geometries and fundamental vibrational wave numbers were calculated using the ab initio (HF) and DFT (B3LYP) gradient methods employing 6-311++G (d,p) basis set. The vibrational frequencies which were determined experimental data are compared with theoretical calculations. The complete assignments are performed on the basis of total energy distribution (TED) of the vibrational modes. The calculated HOMO-LUMO energy gap reveals that the charge transfer occurs within the molecule. Thermo dynamical properties like entropy, heat capacity, zero-point vibrational energy and Mulliken's charge analysis have been calculated for CHNP. The most possible interaction is explained using nature bond orbital (NBO) analysis and the potential compound of non-linear optics (NLO) demands the investigation of its structural and bonding features contributing the hyperpolarizability. The optimized geometrical parameters, fundamental vibrational frequencies, IR intensity, Raman activity are calculated using the GAUSSIAN 09W program packages. The molecular docking results were clustered together and represented by the result with the most favourable free energy of binding.

1. Introduction

The pyridine derivatives have an important position in the heterocyclic compounds and are importantin bactericidal, fungicidal, germicidal and pharmacological activities, and they can be used as nonlinear materials and photo chemicals. Pyridines are widely used in pharmacological and medical applications. Some of them show anaesthetic properties and have been used as drugs for certain brain diseases. Pyridine tagged oligosaccharides have been widely used for sensitive qualitative and quantitative analysis by high performance liquid chromatography with fluorescence detection [1-3]. Pyridine is used in preparation of cytidineanalogs [4] and it is also immensely used as a reagent in analytical chemistry. The vibrational spectra of 4-hydroxy pyridine have been investigated by several authors [5-7]. Extensive research in the last decade has shown that organic compounds often possess a higher degree of optical non-linearity than their inorganic counterparts. Based on the literatures [8–10] supported by data banks [11-17] of various national and international journals an attempt has been made in this study to interpret the vibrational spectra of 5-chloro-2-hydroxy-3-nitropyridine (CHNP)by combining the experimental and theoretical information using density functional theory (B3LYP) to derive information about electronic effects and intramolecular charge transfer responsible for biological activity. The HOMO–LUMO energy gap have been constructed at B3LYP/6-311++G(d,p) level to understand the electronic properties, electrophilic and nucleophilic active centres of CHNP.

2. Experimental and computational methods

2.1. Experimental Methods

The pure sample of5-chloro-2-hydroxy-3-nitropyridine (CHNP) was obtained from Lancaster chemical Company, UK and used for recording the spectra as such without any further purification. The FT-IR spectrum of CHNP was measured in the BRUKER IFS 66V spectrometer in the range 4000–400 cm^{-1}. The FT-Raman spectrum of 5-chloro-2-hydroxy-3-nitropyridine was also recorded in FT-RamanBRUKER RFS 100/s instrument equipped with Nd:YAG laser source operating at 1064 nm wavelength and 150 mW power. The spectrum was recorded in the range 3500–50 cm^{-1}. The spectral resolution is ± 1 cm^{-1}.

2.2. Methods of Computation

The initial geometry of CHNP is optimized using the HF/6–311++G(d,p) and B3LYP/6–311++G(d,p) level of GAUSSIAN 09W programme package [18]. The vibrational frequency analysis is computed using HF/6–311++G(d,p) and B3LYP/6–311++G(d,p) level method to determine the nature of a stationary point found by geometry optimization. The first hyperpolarizability of the atoms of CHNP have been calculated using HF/6–311++G(d,p) and B3LYP/6–311++G(d,p)level methods. The HOMO–LUMO analysis has been carried out to explain the charge transfer within the compound. The chemical hardness (η) and chemical potential (μ) have been calculated using the highest occupied molecular orbital (HOMO) and lowest unoccupied molecular orbital

Table 1. Optimized geometrical parameters of 5-Chloro-2-Hydroxy-3-Nitropyridine obtained by B3LYP/6-311++G (d,p) and HF/6-311++G (d,p) methods.

Bond Length	Values		Bond Angle	Values		Dihedral Angle	Values	
	B3LYP	HF		B3LYP	HF		B3LYP	HF
	6-311++ G (d,p)	6-311++ G (d,p)		6-311++ G (d,p)	6-311++ G (d,p)		6-311++ G (d,p)	6-311++ G (d,p)
N1-C2	1.3302	1.312	C2-N1-C6	120.004	120.1297	C6-N1-C2-C3	0.2435	0.1212
N1-C6	1.3309	1.3175	N1-C2-C3	120.9689	120.855	C6-N1-C2-O7	178.5382	178.3633
C2-C3	1.4087	1.3992	N1-C2-O7	117.3277	117.4859	C2-N1-C6-C5	-0.9318	-0.8696
C2-O7	1.3353	1.3143	C3-C2-O7	121.6808	121.635	C2-C1-C6-H11	179.2682	179.4102
C3-C4	1.3883	1.378	C2-C3-C4	119.3067	119.3124	N1-C2-C3-C4	0.9818	1.0871
C3-N8	1.4743	1.4577	C2-C3-N8	122.9688	122.9476	N1-C2-C3-N8	-179.3468	-179.1106
C4-C5	1.3868	1.3787	C4-C3-N8	117.7237	117.7397	O7-C2-C3-C4	-177.2379	-177.0814
C4-H9	1.0814	1.0719	C3-C4-C5	118.5963	118.6199	O7-C2-C3-N8	2.4355	2.721
C5-C6	1.3929	1.3792	C3-C4-H9	119.3488	119.7073	N1-C2-O7-H12	-0.4687	-0.0457
C5-Cl10	1.747	1.7347	C5-C4-H9	122.0549	121.6723	C3-C2-O7-H12	177.813	178.1819
C6-H11	1.0845	1.0748	C4-C5-C6	118.7394	118.251	C2-C3-C4-C5	-1.5006	-1.533
O7-H12	0.9691	0.9455	C4-C5-Cl 10	120.9394	121.0989	C2-C3-C4-H9	178.5126	178.7253
N8-O13	1.2267	1.1916	C6-C5-Cl 10	120.3211	120.65	N8-C3-C4-C5	178.8109	178.6544
N8-O14	1.2193	1.1811	N1-C6-C5	122.3663	122.8133	N8-C3-C4-H9	-1.1759	-1.0873
			N1-C6-H11	116.9224	116.662	C2-C3-N8-O13	-155.9818	-155.3507
			C5-C6-H11	120.711	120.524	C2-C3-N8-O14	25.1951	26.0227
			C2-O7-H12	106.6297	108.4133	C4-C3-N8-O13	23.6945	24.4545
			C3-N8-O13	116.6703	116.4976	C4-C3-N8-O14	-155.1286	-154.172
			C3-N8-O14	117.9723	118.2195	C3-C4-C5-C6	0.8547	0.8323
			O13-N8-O14	125.3457	125.267	C3-C4-C5-Cl10	-179.2394	-179.2603
						H9-C4-C5-C6	-179.1589	-179.4313
						H9-C4-C5-Cl10	0.7469	0.476
						C4-C5-C6-N1	0.3711	0.3793
						C4-C5-C6-H11	-179.8363	-179.9109
						Cl 10-C5-C6-N1	-179.5353	-179.5285
						Cl 10-C5-C6-H11	0.2573	0.1812

(LUMO). The comparison between the calculated and the observed vibrational spectra helps us to understand the observed spectral features. In order to improve the agreement of theoretically calculated frequencies with experimentally calculated frequencies, it is necessary to scale down the theoretically calculated harmonic frequencies. Hence, the vibrational frequencies calculated at HF/6–311++G(d,p) and B3LYP/6–311++G(d,p)levels are scaled down by using MOLVIB 7.0 version written by Tom Sundius [19,20,21].

2.3. Prediction of Raman Intensities

The Raman activities (S_i) calculated by GAUSSIAN 09W package have been suitably adjusted by the scaling procedure with MOLVIB program and subsequently converted to relative Raman intensities (I_i) using the following relationship derived from the basic theory of Raman scattering [22-24].

$$I_i = \frac{f(\nu_0 - \nu_i)^4 S_i}{\nu_i\left[1 - \exp\left(-\frac{hc\nu_i}{kT}\right)\right]} \quad \ldots (1)$$

whereν_0 is the exciting frequency in cm^{-1}, $\nu_i$is the vibrational wavenumber of the i^{th} normal mode, h, c and k are the fundamental constants and f is a suitably chosen common normalization factor for all the peak intensities.

3. Results and discussion

3.1. Optimized Geometry

The optimized molecular structure with numbering scheme of CHNP is shown in Fig.1. The geometry of the compound under investigation is considered by possessing C_1 point group symmetry. The calculated optimized geometrical parameters of CHNP by HF/6–311++G(d,p) and B3LYP/6–311++G(d,p) levels are presented in Table.1. Detailed description of vibrational modes can be given by means of normal coordinate analysis.

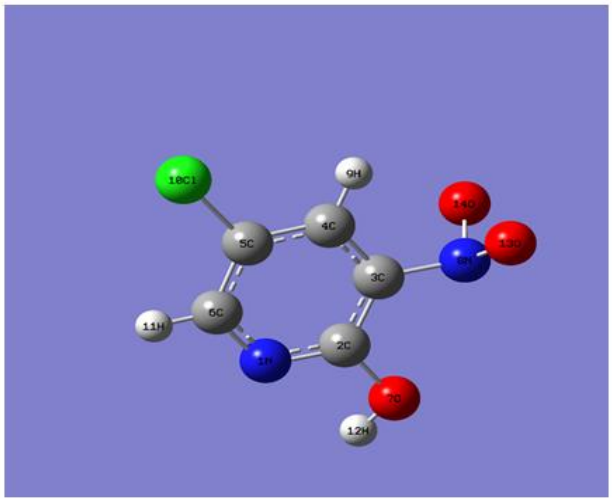

Fig 1.Optimized molecular structure of 5-Chloro-2-Hydroxy-3-NitroPyridine.

4. Vibrational frequency analysis

The molecule consists of 14 atoms and expected to have 36 normal modes of vibrations. The symmetry of the molecule is considered as C_1. All the 36 normal modes of vibrations, belonging to species A. These modes are found to be IR and Raman active suggesting that the molecule possesses a non-centro symmetric structure, which recommends the investigated compound for non-linear optical applications. The experimentally and theoretically calculated IR, Raman frequencies are presented in Table.2. The FT-IR and FT-Raman spectra of the CHNP are shown in Fig. 2 and 3 respectively.

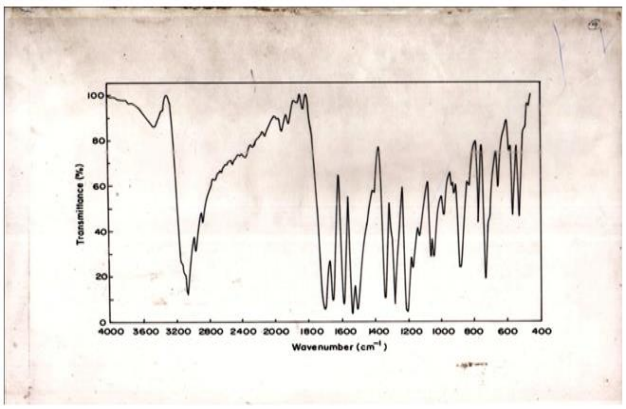

Fig 2. FT-IR Spectrum of 5-Chloro 2-Hydroxy-3-Nitropyridine.

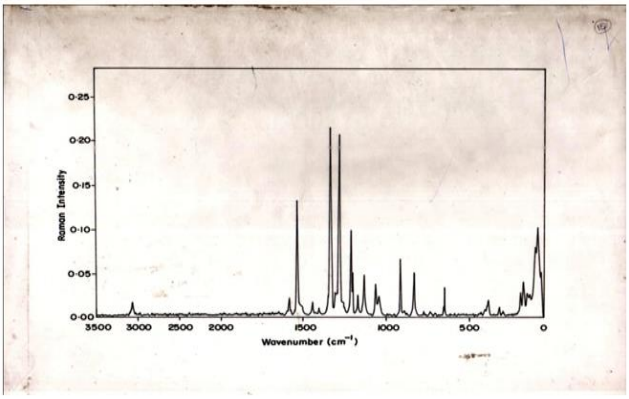

Fig 3. FT-Raman Spectrum of 5-Chloro 2-Hydroxy-3-Nitropyridine.

C–C vibrations

The bands observed at 1650–1400 cm^{-1} are assigned to C–C stretching modes good group vibrations [25] with heavy substituents, the bonds tend to shift to somewhat lower wavenumbers and greater the number of substituents on the ring, broader the absorption regions. As predicted in the earlier references, in CHNP the C–C stretching vibrations observed at 1589, 1538, 1404, 1340 cm^{-1} in FT-IR and vibrations observed at 1586, 1540, 1403, 1339 cm^{-1} in FT-Raman. The C–C in-plane and out-of-plane bending modes of CHNP are summarized in Table 2.

C–N vibrations

The C–N stretching frequencies in the side chain are a rather difficult task, since there are problems in identifying these frequencies from other vibrations. The C–N stretching usually lies in the region 1400–1200 cm^{-1}. Since, mixing of bands is possible in this region. However, with the help of force field calculations the C–N vibrations are identified [26]. In this investigation, the C–N stretching vibrations of CHNP are found at 1230, 1205 cm^{-1} in FT-IR and at 1283, 1204, cm^{-1}in FT-Raman spectrum. The C–N bending vibrations and deformations of CHNP are summarized in Table 2.

C–H vibrations

The hetero aromatic structure shows the presence of C–H stretching vibrations in the region 3100–3000 cm^{-1} [27, 28, 29]. This is the characteristic region for the ready identification of C–H stretching vibrations. In this region, the bands are not affected appreciably by the nature of the substitutions. In the present investigation, the C–H vibrations are observed at 3070 and 2967 cm^{-1} in the FT-IR spectrum and at 3069 cm^{-1} in the Raman for CHNP.

Table 2 . The observed (FT-IR & FT-Raman) calculated (Unscaled and Scaled) frequencies (cm-1) and probable assignments (characterized by TED) of 5-Chloro 2-Hydroxy-3-Nitropyridine.

S.NO	Observed Frequencies		Calculated Values				TED% Among Types Internal Co-Ordinates
	FT-IR	FT-Raman	B3LYP/6- 311 + + G (d,p)		HF/6-311 + + G (d,p)		
			Frequencies		Frequencies		
			Unscaled	Scaled	Unscaled	Scaled	
1	3445	_	3756	3050	4123	3453	γ O-H (99%)
2	3070	3069	3224	3074	3395	3079	γ C-H (98%)
3	2967	_	3183	2970	3357	2977	γ C-H(97%)
4	1654	_	1648	1656	1843	1665	NO2 assy (96%)
5	1608	_	1614	1610	1784	1620	NO2 symm (95%)
6	1589	1586	1586	1592	1770	1597	γ C-C (76%)
7	1538	1540	1485	1542	1626	1547	γ C-C (80%)
8	1404	1403	1435	1409	1620	1414	γ C-C (85%)
9	1340	1339	1372	1342	1552	1351	γ C-C (83%)
10	_	1283	1342	1286	1461	1295	γ C-N (80%)
11	1230	_	1333	1234	1433	1238	γ C-N (82%)
12	1205	1204	1274	1210	1313	1214	γ C-N (81%)
13	1172	1173	1188	1177	1248	1182	γ C-O (79%)
14	1131	1136	1123	1139	1218	1143	b O-H (78%)
15	1063	1066	1098	1073	1181	1076	b C-H(76%)
16	1043	1047	961	1069	1098	1057	b C-H(75%)
17	981	_	932	986	1062	996	b C-C(74%)
18	932	_	928	937	1023	944	b C-C(73%)
19	918	917	845	922	932	931	b C-N(72%)
20	882	_	782	884	886	896	b C-N(71%)
21	_	834	745	839	834	849	b C-N(70%)
22	829	_	716	835	791	841	b NO2(68%)
23	775	_	666	782	720	788	b NO2(65%)
24	731	_	582	736	635	741	γ C-Cl (60%)
25	656	651	557	666	598	671	ω O-H (58%)
26	588	_	522	599	540	604	ω C-H (57%)
27	565	_	445	577	484	582	ω C-H (56%)
28	527	_	407	537	445	545	ω C-C (55%)
29	468	_	389	479	424	487	ω C-C (54%)
30	410	_	375	422	409	430	ω NO2 (53%)
31	_	385	332	386	364	400	ω NO2 (52%)
32	_	319	275	327	301	331	b C-Cl (51%)
33	_	192	175	212	191	208	ω C-N (50%)
34	_	175	148	185	166	192	ω C-N (48%)
35	_	151	106	162	124	170	ω C-N (47%)
36	_	86	39	98	48	106	ω C-Cl (46%)

Abbreviations: γ – stretching; b – bending; ω– out-of-plane bending; t – torsion; R – ring; trigd – trigonal deformation; symd – symmetric deformation; asymd – antisymmetric deformation.

The C–H in-plane and out-of-plane bending vibrations of the CHNP have also been identified and listed in Table 2.

O–H vibrations

The precise positions of O–H band are dependent on the strength of hydrogen bond. The O–H stretching vibration is normally observed at about 3350 cm^{-1}. The O–H in-plane bending vibration is observed in the region 1440–1260 cm^{-1} [30]. In CHNP, the bands appeared at 3445 cm^{-1} in FT-IR spectrum were assigned to O–H stretching modes of vibrations. The in-plane bending vibrations of hydroxy groups have been identified at 1131 cm^{-1}, in IR spectrum. The O–H out-of-plane vibrations of the title compound have also been identified and listed in Table2.

C-Cl vibrations

The C–Cl stretching vibrations generally give strong bands in the region 760-505 cm^{-1} [31]. The FT-IR band observed at 731 cm^{-1} has been assigned to C–Cl stretching; this was also confirmed by TED output. Most of the aromatic chloro compounds have a band of strong-to- medium intensity in the region 385–265 cm^{-1} due to C–Cl in-plane bending vibrations [272]. Accordingly the FT-Raman band identified at 319 cm^{-1} has been assigned to the C–Cl in-plane bending mode. The C–Cl out of plane deformation vibration has been established at 86 cm^{-1} in FT-Raman spectrum.

NO_2 group vibrations

The characteristic group frequencies of the nitro group are relatively independent of the rest of the molecule which makes this group convenient to identify. Aromatic nitro compounds have strong absorptions due to the asymmetric and symmetric stretching vibrations of the NO_2 group at 1570–1485 cm^{-1} and 1370–1320 cm^{-1}, respectively [33]. Hence, the asymmetric stretching mode of nitro group for CHNP is identified at 1654 cm^{-1} in FT-IR spectra are in good agreement with TED output. The symmetric stretching mode of nitro group is assigned at 1608 cm^{-1} in IR spectra ofCHNP. The NO_2 scissoring mode for CHNP has been designated to the bands at 734 and 742 cm^{-1} in IR and Raman spectra, respectively. The scissoring modes of NO_2 group for CHNP has been designated to the peak at 829 $cm^{-1}$and 775 cm^{-1} in IR spectrum. The deformation vibrations of NO_2 group (rocking, wagging and twisting) contribute to several normal modes in the low frequency region [34]. These bands are also found well within the characteristic region and summarized in Table2 for CHNP.

5. First hyperpolarizability

The first hyperpolarizability (β_0) of these novel molecular system and the related properties (β_0, α_0) of CHNP have been calculated based on the finite field approach. In the presence of an applied electric field, the energy of a system is a function of the electric field. The first hyperpolarizability is a third - rank tensor that can be described by a $3 \times 3 \times 3$ matrix. The 27 components of the 3D matrix can be reduced to 10 components due to Kleinman symmetry [35]. It can be given in the lower tetrahedral. The components of β are defined as the coefficients in the Taylor series expansion of the energy in the external electric field. When the external electric field is weak and homogenous, this expansion becomes,

$$E = E^\circ - \mu_\alpha F_\alpha - \frac{1}{2}\alpha_{\alpha\beta} F_\alpha F_\beta - \frac{1}{6}\beta_{\alpha\beta\gamma} F_\alpha F_\beta F\gamma + \ldots \quad \ldots (2)$$

where E° is the energy of the unperturbed molecules, F_α the field at the origin and μ_α, $\mu_{\alpha\beta}$ and $\beta_{\alpha\beta\gamma}$ are the components of dipole moment, polarizability and the first hyperpolarizabilities, respectively. The total static dipole momentμ, the mean polarizability α_0, the anisotropy of the polarizability β_0, using the x, y, z components they are defined as follows.

$\mu = (\mu_x^2 + \mu_y^2 + \mu_z^2)^{1/2}$

$\alpha_0 = \dfrac{\alpha_{xx} + \alpha_{yy} + \alpha_{zz}}{3}$

$\alpha = 2^{-1/2}[(\alpha_{xx} - \alpha_{yy})^2 + (\alpha_{yy} - \alpha_{zz})^2 + (\alpha_{zz} - \alpha_{xx})^2 + 6\alpha_{xx}^2]^{1/2}$

$\beta_0 = (\beta_x^2 + \beta_y^2 + \beta_z^2)^{1/2}$

and

$\beta_x = \beta_{xxx} + \beta_{xyy} + \beta_{xzz}$

$\beta_y = \beta_{yyy} + \beta_{xxy} + \beta_{yzz}$

$\beta_z = \beta_{zzz} + \beta_{xxz} + \beta_{yyz}$

For CHNP the total molecular dipole moment (μ) is 4.2398 and 3.9601 Debye byHF/6-311++G(d,p) and B3LYP/6-311++G(d,p) methods, respectively. Mean first hyperpolarizability (β) is 1.2355 $\times 10^{-30}$ esu and 2.5600 $\times 10^{-30}$ esu by HF/6-311++G(d,p) and B3LYP/6-311++G(d,p) methods, respectively. The first hyperpolarizability of CHNPis six times more than those of urea (μ and β of urea are 1.3732 Debye and 0.3728×10^{-30} esu).

Table 3.The Thermodynamic parameters of 5-Chloro-2-Hydroxy-3-Nitropyridinecalculated by HF and B3LYP methods.

Parameters	Method/Basis Set	
	B3LYP	HF
	6-311++G (d, p)	6-311++G (d, p)
Total Energy Etotal	59.406	63.913
Heat Capacity (Cv)	32.895	30.629
Entropy (S)	96.037	93.331
Translational	0.889	0.889
Rotational	0.889	0.889
Vibrational	57.629	62.136
Zero Point vibrational Energy	53.74081	58.61719
Rotational Constant(GHZ)		
A	1.70765	1.751
B	0.65972	0.67231
C	0.48157	0.49175
Dipole Moment		
µx	-2.9839	-3.1478
µy	2.6025	2.8398
µz	-0.0764	-0.0501
µtotal	3.9601	4.2398
Molecular mass	173.98322 amu	173.98322 amu
Rotational Temperature (Kelvin)		
T1	0.08195	0.08403
T2	0.03166	0.03227
T3	0.02311	0.0236

6. HOMO–LUMO Analysis

The frontier molecular orbital pictures for CHNP are shown in Fig. 4. The orbital determine the way in which the molecule interacts with other species. HOMO is the orbital that acts as an electron donor, and LUMO is the orbital that acts as an electron acceptor. HOMO–LUMO helps to characterize the chemical reactivity and kinetic stability of the molecule . A molecule with a small gap is more polarized and is known as soft molecule. Low value of energy gap is also due to electron withdrawing groups that enter into conjugation. The strongest bands in the IR spectra are weak in Raman spectra and vice versa, but the intermolecular charge transfer from the donor to acceptor group can induce large variations of the molecular polarizability of both IR and Raman activities at the same time. The LUMO, of π nature, is molecular delocalized over the whole C–C bond. By contrast,

the HOMO is located over chlorine atoms and amino groups; consequently the HOMO–LUMO transition implies an electron density transfer to pyridine ring of π conjugated system from chlorine atoms and amino groups. Moreover, these three orbitals significantly overlap in the different positions of the pyridine ring for CHNP reflect the chemical activity of the molecule.

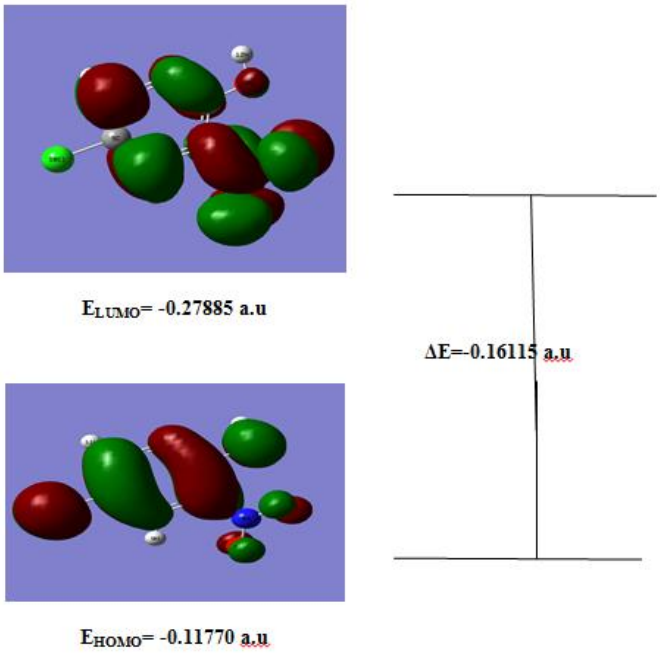

Fig 4. HOMO and LUMO plot of 5-Chloro-2-Hydroxy-3-NitroPyridine.

The calculated self-consistent field (SCF) energy of CHNP is -987.67322 a.u by B3LYP/6-311++G(d,p) and -983.92417 a.u. by HF/6-311++G(d,p) methods. The B3LYP is a popular and efficient exchange correlation functional for calculating energies and geometries, it has been proven to be able to yield reliable results for small molecules [36]. Global hardness (η), Electronic chemical potential (μ) Electrophilicity index (ω), Ionization energy (I) and Electron affinity (A) of CHNP are calculated by B3LYP/6-311++G(d,p) and HF/6-311++G(d,p) methods are listed in Table. 4

Table 4. HOMO-LUMO energy gap and related molecular properties of 5-Chloro-2-Hydroxy-3-Nitropyridine.

Global Descriptors	Method/Basis Set	
	B3LYP/6-311++G (d, p)a.u	HF/6-311++G (d, p)a.u
HOMO Energy	-0.27885	-0.36798
LUMO Energy	-0.11770	0.03091
Energy Gap	-0.16115	-0.39889
Ionisation Potential (I)	0.27885	0.36798
Electron Affinity (A)	0.11770	-0.03091
Chemical Potential(μ)	-0.19827	-0.168535
Hardness (η)	0.22	0.38343
Global electroplicity (ω)	0.08934	0.03703
Softness (s)	4.5454	2.60803
Electro negativity (χ)	0.39655	0.168535

7. Mulliken atomic charges

Mulliken atomic charge calculation [37] has an important role in the application of quantum chemical calculation to molecular system, because atomic charges affect dipole moment, polarizability, electronic structure, and much more properties of molecular systems. The total atomic charges of CHNP obtained by Mulliken population analysis with DFT (B3LYP) with 6-311++G(d,p) and HF/6-311++G(d,p) basis sets are listed in Table 5. The negative values on C2, C3, N1, C6, O7, N8 and O13 atom in the aromatic ring lead to a redistribution of electron density. Due to this strong negative charges, C4, C5, H9, Cl10, H11, H12 and O14 accommodate higher positive charge and becomes more acidic. In the pyridine ring all the hydrogen atoms have a net positive charge, in particular, the hydrogen atom Cl10 and H12 have charge of 0.417469 and 0.304142 a.u., respectively. The better represented graphical form of the results has been done in Fig.5.

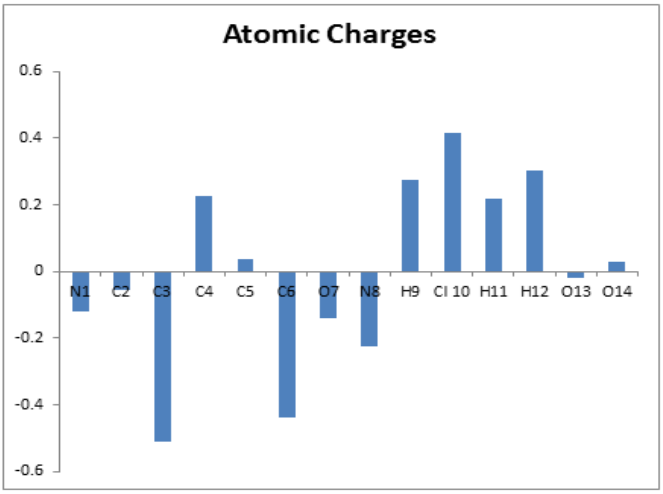

Fig 5. Plot of Mulliken's atomic charges of 5-Chloro-2-Hydroxy-3-Nitropyridine.

8. NBO Analysis

The interactions between the orbitals can be interpreted through NBO theory. NBO theory allows the assignment of the hybridization of atomic lone pairs and of the atoms involved in bond orbitals. These are the important data in spectral interpretation since the frequency ordering is related to the bond hybrid composition [38].

The natural bond orbital analyses provides an efficient method for studying intra and inter molecular bonding and interaction among bonds and also provides a convenient basis for investigating charge transfer (or) conjugative interaction in molecular systems. Some electron donor orbital, acceptor orbital and the interacting stabilization energy resulting from the second–order micro disturbance theory reported [39-40]. The result of interaction is a loss of occupancy from the concentration of electron NBO of the idealized Lewis structure in to an empty non–Lewis orbital. For each donor (i) and acceptor (j), the stabilization energy E(2) associated with delocalization $i \rightarrow j$ is estimated as,

$$E(2) = -n_\sigma \frac{\langle \sigma | F | \sigma \rangle^2}{\varepsilon_\sigma^* - \varepsilon_\sigma} = -n_\sigma \frac{F_{ij}^2}{\Delta E} \qquad \ldots (3)$$

where $\langle \sigma | F | \sigma \rangle^2$ (or) F_{ij}^2 is the Fock matrix element i and j NBO orbitals, ε_σ and ε_σ^* are the energies of σ and σ* NBO's and n_σ is the population of the donar σ orbital.

Larger the E(2) value, the interaction between electron donors and electron acceptors is more intensive and greater the extent of conjugation of whole system.

Table 6.Second order perturbation theory analysis of Fock matrix in NBO basic corresponding to the intermolecular bonds of 5-chloro-2-Hydroxy-3- Nitropyridine.

DONOR	TYPE	OCCUPANCY	ACCEPTOR	TYPE	OCCUPANCY	E(2)	Ej-Ei	F (i,j)
N1-C2	σ	1.98467	C3-N8	σ*	0.0305	2.68	1.1	0.049
	π	1.7056	C5-C6	π *	0.40478	26.35	0.31	0.082
N1-C6	σ	1.97655	C2-O7	σ*	0.01363	3.63	1.09	0.057
C2-C3	σ	1.98145	C3-C4	σ*	0.04381	3.56	1.28	0.06
C2-O7	σ	1.99101	N1-C6	σ*	0.04657	1.96	1.35	0.046
C3-C4	σ	1.96077	N8-O14	π *	0.02059	1.3	0.65	0.03
	π	1.66177	N1-C2	π *	0.35623	27.35	0.27	0.078
C3-N8	σ	1.98438	N8-O14	π *	0.06216	0.55	0.74	0.021
C4-C5	σ	1.97502	C3-N8	σ*	0.0263	4.63	1.01	0.061
C4-H9	σ	1.9746	C5-H6	σ*	0.01149	3.72	1.07	0.057
C5-C6	σ	1.98628	C4-C5	σ*	0.03613	2.73	1.28	0.053
	π	1.62756	C3-C4	π *	0.35426	25.35	0.28	0.076
C5-Cl10	σ	1.98778	N1-C6	σ*	0.03096	2.25	1.23	0.047
C6-H11	σ	1.98234	N1-C2	σ*	0.02201	4.07	1.05	0.058
O7-H12	σ	1.97394	N1-C2	π *	0.00575	4.08	0.71	0.053
N8-O13	σ	1.98752	C2-C3	σ*	0.06611	0.92	1.4	0.032
N8-O14	π	1.9859	C3-C4	π *	0.16591	3.71	0.51	0.042
N1-C2	π *		C5-C6	π *	0.40478	277.06	0.01	0.08
N8-O14	σ*		C3-N8	σ*	0.16591	1.62	0.14	0.04
	π *		N8-O14	σ*	0.54694	72.49	0.21	0.184
LP(1) N1	n1 N1		C5-C6	σ*		8.18	0.87	0.077
LP(2) O7	n2 O7		N1-C2	σ*		7.72	0.92	0.076
LP(3) O13	n3 O13		N8-O14	π *		55.04	0.2	0.094

E(2) means energy of hyper conjugative interaction (stabilization energy).
Energy difference between donor and acceptor i and j NBO orbitals.
F(i,j) is the Fock matrix element between i and j NBO orbitals.

The intra–molecular hyperconjugative interactions are formed by the orbital overlap between π (C–C) and germinal π*(C–C) bond orbitals which results in intra-molecular charge transfer (ICT) causing stabilization of the system are presented in Table 6. NBO analysis reveals the charge transfer interaction between the electron donating methyl groups and the germinal σ*(C–C) orbitals. In FMQ, the intramolecular hyperconjugative interaction of π^*(N1–C2) → π^*(C5–C6)leading the stabilization of 277.06 kJ/mol, respectively. Similarly the intramolecular hyperconjugative interaction of π^*(N8–O14) → π^*(N8-O14) and LP(3)O13→ π^*(N8-O14) leading to stabilization of 72.49 and 55.04 kJ/mol, respectively. The intramolecular interaction are formed by the orbital overlap between bonding C–C, C–N and C–H antibond orbital which results intramolecular charge transfer (ICT) causing stabilization of the system. These interactions are observed as increase in electron density (ED) in C–C, C–N antibonding orbital that weakens the respective bonds.

The energies for the interaction n1(N1) → σ^*(C5-C6) and n2(O7) → σ^*(N1–C2) are 8.18 and 7.72 kJ mol^{-1}, respectively which clearly demonstrate the intramolecular hyperconjugative interaction between the N–C and C–C and N-O group is strong in the ground state for FMQ.

9. Antibacterial activity of synthetic compounds

9.1. Material method - Protein preparation

AutoDock is a suite of automated docking tool. It is designed to predict how small molecules, such as substrates or drug candidates, bind to a receptor of known 3D structure (41). The protein structures' retrieved from PDB database. The protein structure of Vibrio cholera BETA-Ketoacyl-(Acyl Carrier Protein) Reductase (PDB ID :(5END) retrieve from protein data bank . All water molecules removed from all protein structure and add with Kollmann charges was assigned. Through which hydrogens were added, side chains were optimized for hydrogen bonding. The energy minimized protein was then saved in PDB format. Using MGLTools-1.4.6 nonpolar hydrogens were merged, AutoDock atom type AD4 and Gasteiger charges were assigned and finally saved in protein.pdbqt format.

9.2. Ligand preparation

Structure of ligands were drawn using ChemSketch (42) , optimized with 3D-geometry and the two-dimensional structure of 5-Chloro-2-Hydroxy 3-Nitro Pyridine is converted into 3-D structure using the open Babel format molecule converter (43) and saved in PDB format for AutoDock compatibility. MGLTools-1.4.6 (The Sripps Research Institute) was used to convert ligand.pdb files to ligand.pdbqt files.

9.3. Active site prediction

The active site of the protein is the binding site or usually a pocket at the surface of the protein that contains residues responsible for substrate specificity which often act as proton donors or acceptors. Identification and characterisation of binding site is the key step in structure based drug design.

Table 7.Molecular docking studies of synthetic compounds with BETA-Ketoacyl- (Acyl Carrier Protein) Reductase for 5-Chloro-2-Hydroxy-3-Nitropyridine.

S. No	Compound name	Docking score	IC_{50} value	H-Bond interaction	Distance
1	5-Chloro-2-Hydroxy Nitro Pyridine	-4	1.9	ARG19 N-H...O ARG19 N-H...O GLY22 N-H...O	2.169 2.657 1.95

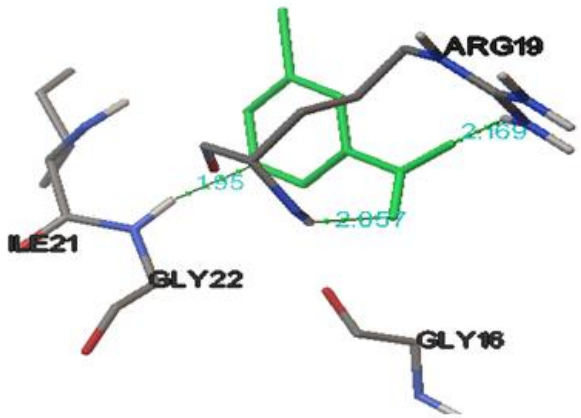

Fig 6. Molecular docking of 5-Chloro-2-Hydroxy-3-Nitropyridine.

The binding site has been identified by computational and literature reports. The active site region of the protein is identified by cast (44). These servers analytically furnish the area and the volume at the probable active site of each pocket to envisage the binding site.

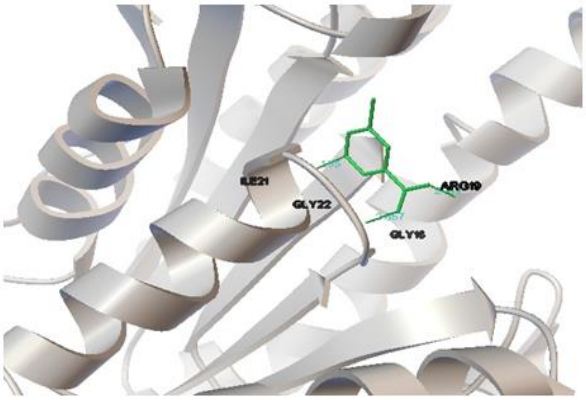

Fig 7. The protein structure of BETA-Ketoacyl (Acyl Carrier Protein) Reductase interact with 5-Chloro-2-Hydroxy-3-NitroPyridine.

9.4. Docking protocol

Grid parameter files (protein.gpf) and docking parameter files (ligand.dpf) have written using MGLTools-1.4.6. Receptor grids were generated using 80x80x60 grid points in xyz with grid spacing of 0.375 Å. Grid box was centered co crystallized ligand map types were generated using autogrid4. Docking of macromolecule was performed using an empirical free energy function and Lamarckian Genetic Algorithm, with an initial population of 250 randomly placed individuals, a maximum number of 106 energy evaluations, a mutation rate of 0.02, and a crossover rate of 0.80. One hundred independent docking runs were performed for each ligand. Results differing by 2.0 Å in positional root-mean square deviation (RMSD) were clustered together and represented by the result with the most favourable free energy of binding**.**

10. Conclusion

The FT-IR and FT-Raman spectra have been recorded and the detailed vibrational assignment of 5-chloro-2-hydroxy 3-nitropyridine is presented for the first time. The equilibrium geometries, harmonic vibrational frequencies of 5-chloro-2-hydroxy-3-nitropyridine are determined and analysedwith HF/6-311++G(d,p) and B3LYP/6-311++G(d,p) levels of theory. The difference between the corresponding wavenumbers (observed and calculated) is very small, for most of fundamentals. Any discrepancy noted between the observed and the calculated frequencies may be due to the fact that the calculations have been actually done on a single molecule in the gaseous state contrary to the experimental values recorded in the presence of intermolecular interactions.Therefore the results presented in this investigation for 5-chloro-2-hydroxy-3-nitropyridineindicate that this level of theory is reliable for prediction of both infrared and Raman spectra of the compound. The present quantum chemical investigation may lead to the understanding of properties and activity of 5-chloro-2-hydroxy-3-nitropyridineand may also help in its use for more advance applications with lesser environmental impairment. The $\mu \times \beta$ value shows that there is a significant increase in optical non-linearities. The HOMO–LUMO energy gap reflects the chemical reactivity of the molecule.The molecular docking results were clustered together and represented by the result with the most favourable free energy of binding**.**

References

[1] M. Okamato, K. Takahashi, T. Doi, Y. Takimoto, Anal. Chem., 69 (1997) 2919.
[2] Z. Dega-Szafran, A. Kania, B. Nowak-Wyadra, M. Szafran, J. Mol. Struct., 322 (1994) 223.
[3] P. Carmona, M. Molina, R. Escobar, Spectrochim., Acta 49A (1993) 1.
[4] S. Hildbrand, A. Blaser, S.P. Parle, C.J. Leman, J. Am. Chem. Soc., 119 (1997) 5499.
[5] D. Gandolfo, J. Zarembowitch, Spectrochim., Acta 33A (1977) 615.
[6] T.K.K. Srinivasan, J. Mol. Liquids, 26 (1983) 177.
[7] O.P. Lamba, J.S. Parihar, H.D. Bist, Y.S. Jain, Indian J. Pure Appl. Phys., 21 (1983) 236.
[8] ReenaRastogi, Ph.D. Thesis (Botony), C.C.S. Univ., Meerut (2003).
[9] R.K. Sharma, Good Manufacturing practices for ISM, Pharmaceuticals, science technology,entrepreneur, 10(18) (1990) 6.
[10] NIOSH and International agency for research on cancer. IARC monographs on the evolutionsof carcinogenic risks to Humans, Printing processes and Printing inks, carbon black and some Nitro compounds, Vol. 65, Lyon, Francel ARC (1996).
[11] The International pharmacopeias, Vol. 5, tests, methods and general requirements, W.H.O. Genevapub. Division (2004).
[12] Basic tests for drugs, W.H.O. Geneva - Pub. Division (2004).
[13] Official methods of microbiological analysis AOAC chemists, Edited by K. Helrich, AOA, Arlington (U.S.A.),(2003).
[14] Official methods of microbiological analysis AOAC group, Vol. 1-3, AOAD, Arlington(U.S.A.),(2003).
[15] The Compendium of analytical methods, Vol. 1-4, evaluation division, bureau of microbiological hazards, food directorate, Health product and food branch, Health Dept.,Canada (2003).
[16] Official methods of microbiological analysis food, Vol. I, evaluation division, Health Dept.,Canada (2003).
[17] Alper, Stanley, manual for therapeutics, J.W. Pub., N. York (1998).
[18] M.J. Frisch, G.W. Trucks, H.B. Schlegal, GAUSSIAN 09, Revision A.02, Gaussian, Inc., Wallingford, CT, 2009.
[19] T. Sundius, Journal of Molecular Structure, 218 (1990) 321.

[20] MOLVIB (V.7.0): Calculation of Hormonic Force Fields and Vibrational Modes of Molecules, QCPE program No. 807 (2002).
[21] T. Sundius, Vibrational Spectroscopy, 29 (2002) 89.
[22] G. Keresztury, S. Holly, J. Varga, G. Besenyei, A.Y. Wang, J.R. Durig, Spectrochim. Acta Part A, 49 (1993) 2007.
[23] P.L. Polavarapu, J. Phys. Chem., 94 (1990) 8106.
[24] G. Keresztury, Raman Spectroscopy: Theory in: J.M. Chalmers, P.R. Griffiths (Ed.), Handbook of Vibrational Spectroscopy, Wiley, 1 (2002).
[25] M. Arivazhagan, V.P. Subhasini, R. Kavitha, R. SenthilkumarSpectrochimica Acta Part A: Molecular and Biomolecular Spectroscopy, Volume 131, 15 October 2014, Pages 636.
[26] Adel S. El-Azab, Y. Sheena Mary, C. YohannanPanicker, Alaa A.-M. Abdel-Aziz, Magda A. El-Sherbeny, C. Van AlsenoyJournal of Molecular Structure, Volume 1113, 5 June 2016.
[27] R.M. Silverstein, G. Clayton Basseler, Morrill, Spectrometric identification of Organic Compounds, John Wiley and Sons, New York, 1991.
[28] G. Varsanyi, Vibrational spectra of 700 Benzene Derivatives, Vol. I-II Academic Kiaclo, Budapest, 1973.
[29] M. Arivazhagan, R. Kavitha, V.P. SubhasiniSpectrochimica Acta Part A: Molecular and Biomolecular Spectroscopy, Volume 130, 15 September 2014, Pages 502.
[30] Jag Mohan, Organic Spectroscopy-Principle and Applications, second ed., Narosa Publishing House, New Delhi, 30.
[31] Yaping Tao, Ligang Han, Xiaofeng Li, Yunxia Han, Zhaojun Liu Journal of Molecular Structure, Volume 1108, 15 March 2016, Pages 307.
[32] E.F. Mooney, Spectrochimica, Acta 20(6) (1964) 1021.
[33] N. Sundaraganesan, S. Ayyappan, H. Umamaheswari, B. Dominic Joshua, Spectrochim., Acta 66A (2007) 17.
[34] A. Kovacs, G. Keresztury, V. Izvekov, Chem. Phys., 253 (2000) 193.
[35] D.A. Kleinman, Phys. Rev., 126 (1962) 1977.
[36] Y. Tao, L. Han, X. Li, Y. Han, et al., Molecular structure, spectroscopy (FT-IR, FTRaman), thermodynamic parameters, molecular electrostatic potential and HOMO-LUMO analysis of 2, 6-dichlorobenzamide, J. Mol. Struct. 1108 (2016) 307.
[37] V.K. Rastogi, M.A. Palafox, L. Mittal, N. Peica, W. Kiefer, k. Lang, P. Ohja, J. RamanSpectrosc., 38 (2007) 1227.
[38] C. James, A. Amal Raj, R. Reghunathan, I. Hubert Jue, V.S. Jayakumar, J. Raman Spectroscopy, 37 (2006) 1381.
[39] L. Jun-na, C. Zhi-Rang, Y. Shen-Fang, J. Zhejiang, Univ. Sci., 68 (2005) 584.
[40] G. Varsanyi, .Assignments for Vibrational Spectra of seven hundred benzene derivatives,Vol. 12, Adam Hilger, 1974.
[41] Morris GM, Goodsell DS, Halliday RS, Huey R, Hart WE, Belew RK, Olson AJ, Automated docking using a Lamarckian genetic algorithm and an empirical binding free energyfunction.J Comp Chem 19 (1998) 1639.
[42] Chem Sketch. ACD – LAB Software for calculating the referred physiochemical parameters. Chem Sketch.
[43] Guha R, Howard MT, Hutchison GR, Murray-Rust P, Rzepa H, Steinbeck C, Wegner J.and WillighagenEL.The blue obelisk-interoperability in chemical informatics.J. Chem.Inf. Model. 46 (2006) , 991.
[44]Andrew Binkowski T, Naghibzadeh S, and Liang J. 2003. CASTp: Computed Atlas ofSurface Topography of proteins. Nucleic Acids Res., 31(13): 3352.